

Distribution of mass in thermal-neutron-induced fission of $^{257}\text{Fm}^\dagger$

K. F. Flynn, J. E. Gindler, and L. E. Glendenin

Chemistry Division, Argonne National Laboratory, Argonne, Illinois 60439

(Received 14 July 1975)

Fission yields were measured radiochemically for mass chains 112, 127, 132, and 140 in thermal-neutron-induced fission of ^{257}Fm . These yields indicate a single-peaked (symmetric) mass distribution. Comparison is made with the distribution deduced from kinetic-energy measurements, and the effects of neutron emission from the fission fragments are considered.

[NUCLEAR REACTIONS, FISSION $^{257}\text{Fm}(n, f)$, $E = 0.025$ eV; measured radio-chemical mass yields.]

INTRODUCTION

Recent calculations¹⁻³ together with experimental observations⁴⁻¹⁰ have indicated a dramatic transition from asymmetric to symmetric mass division as the most probable mode of fission in fermium isotopes of mass 254 through 258. Thus the "provisional" mass distributions derived from kinetic-energy measurements of coincident fragments (shown in Fig. 1) are double peaked for ^{254}Fm ⁴ and ^{256}Fm ⁷ spontaneous fission (sf), characteristic of asymmetric mass splits. They are nearly single peaked for $^{257}\text{Fm}(sf)$ ^{5,6} and ^{255}Fm ⁸ thermal-neutron-induced fission (n, f), indicative of significant amounts of symmetric mass splitting. They are single peaked for $^{257}\text{Fm}(n, f)$ ⁶ denoting that symmetric mass division is the most probable mode of fission for this system. It should be emphasized that provisional mass distributions are not corrected for the effect of neutron emission on the kinetic energies of the fission fragments. Without this correction the shape of the primary (pre-neutron-emission) fragment mass distribution is not determined unambiguously. The neutron yield as a function of primary fragment mass $\bar{\nu}(M)$ has not been measured directly for fission of any of the fermium isotopes. Such functions have been determined, however, for $^{233}\text{U}(n, f)$,^{11,12} $^{235}\text{U}(n, f)$,¹¹⁻¹⁷ $^{239}\text{Pu}(n, f)$,^{12,14} and $^{252}\text{Cf}(sf)$.¹⁸⁻²⁴ The shapes of these functions are characteristically *saw toothed*. Similar saw-tooth-shaped functions have been deduced for $^{245}\text{Cm}(n, f)$,²⁵ $^{254}\text{Cf}(sf)$,²⁶ $^{254}\text{Es}(n, f)$, and $^{256}\text{Fm}(sf)$ ⁷ by a modification⁷ of the Terrell method²⁷ which compares cumulative yields from the primary mass distribution with those yields from the secondary (post-neutron-emission) mass distribution for a given fissioning system. The primary mass distribution determined for $^{256}\text{Fm}(sf)$ is double peaked, characteristic of asymmetric mass division, with either the deduced saw-toothed $\bar{\nu}(M)$ or a fictive, flat $\bar{\nu}(M)$ used to correct the provisional mass dis-

tribution, although the saw-toothed function results in a deeper valley in the mass distribution. If, however, a saw-toothed $\bar{\nu}(M)$ is used to correct provisional mass distributions for $^{257}\text{Fm}(sf)$ or $^{255}\text{Fm}(n, f)$ the resulting primary mass distributions are double peaked and for $^{257}\text{Fm}(n, f)$ may even be triple peaked.⁶

Secondary-fragment mass distributions have been determined radiochemically for $^{254}\text{Fm}(sf)$,^{7,10} $^{256}\text{Fm}(sf)$,⁹ and $^{255}\text{Fm}(n, f)$.⁷ Each of these distributions (shown in Fig. 2) is double peaked, characteristic of primarily asymmetric mass division, although the peak-to-valley ratio decreases significantly⁷ from ~60 to 12 to 2.5, respectively, for these fissioning systems. Also, both the light and heavy mass peaks for $^{255}\text{Fm}(n, f)$ are shifted toward symmetry. This is in contrast to most other systems that fission asymmetrically. For such systems the heavy-mass peak position is relatively stationary, and the light-mass peak shifts accord-

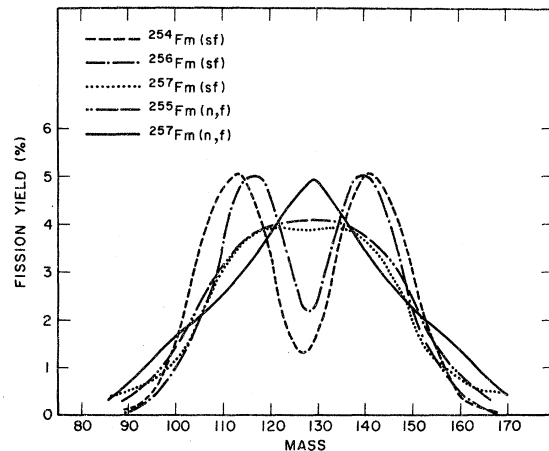


FIG. 1. Provisional mass distributions for fission of various fermium isotopes derived from kinetic-energy measurements of coincident fission fragments. (The distributions are "provisional" since no correction was made for neutron emission by the fragments.)

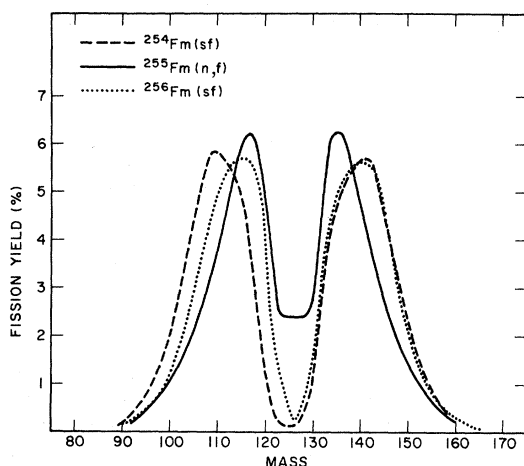


FIG. 2. Secondary mass distributions for fission of various fermium isotopes determined through radiochemistry and γ -ray spectrometry.

ing to the mass of the system. Since the symmetric or asymmetric character of the mass distributions for fission of the fermium isotopes is of considerable theoretical importance, we have investigated the mass distribution for $^{257}\text{Fm}(n,f)$ radiochemically.

EXPERIMENTAL

A sample of approximately 10^9 atoms of ^{257}Fm was obtained through the Heavy Element Program from Oak Ridge National Laboratory. The fermium was separated from contaminating elements (especially from actinide and fission product elements) by passing it through a cation exchange column using α -hydroxyisobutyric acid as the eluting agent and an extraction chromatographic column using di(2-ethylhexyl) orthophosphoric acid (HDEHP) as the stationary phase.²⁸

A ^{257}Fm source was prepared by depositing the purified fermium in solution onto a high-purity quartz disk (1 mm thick by 1.6 cm diam) that had been etched with hydrofluoric acid, washed with triply distilled water, and washed again in the elutriant of the HDEHP column after the fermium had been eluted. The fermium solution was then evaporated to dryness with an induction heater.

The ^{257}Fm source was sandwiched between two identical quartz disks on either side serving as fission product recoil catcher, blank, and guard foils. This target assembly was wrapped in aluminum foil, placed in an aluminum canister, and irradiated in the central thimble of the Argonne heavy-water reactor (CP-5) for periods of three to seven days. The neutron flux ϕ in this position was $\sim 6 \times 10^{13}$ neutrons $\text{cm}^{-2} \text{sec}^{-1}$. After irradiation the catcher and blank foils were separately

etched in an HF-HNO_3 acid solution for a period (~ 10 min) sufficient to completely remove the fission products as shown by tests with $^{252}\text{Cf}(sf)$. The foil adjacent to the back side of the fermium source served as the blank for any induced activities other than those attributable to $^{257}\text{Fm}(n,f)$.

The saturated fission product activity expected from 10^9 atoms of ^{257}Fm assuming a fission cross section of 2950 b²⁹ and a 1% fission yield is about 100 dis/min. After allowing for collection efficiency, saturation factors, chemical yield in the radiochemical separation, and β counting efficiency, one would expect to detect about 10 counts/min. This expected low counting rate demanded that the catcher foils be extremely pure with respect to elements in the fission product region ($Z \sim 35$ through 65) as well as actinide contaminants (particularly ^{235}U). Several materials were tested for this purpose: high-purity quartz and aluminum, zone-refined silicon, polyimide, polyethylene, and coatings of lead oxide. Although superior in terms of induced activity, the polyethylene foils deteriorated severely after a few hours irradiation, even in a lower flux (2×10^{13} neutrons $\text{cm}^{-2} \text{sec}^{-1}$). None of the other materials, including that selected for use (high-purity quartz), was sufficiently free from neutron-induced contaminant activities to permit radiochemical determination of many of the fission product yields. It was therefore possible to determine only the yields of those fission product nuclides which could not be formed by first-order neutron capture by stable nuclides but could be measured via daughter activities. Accordingly, samples of palladium, antimony, tellurium, and barium were initially separated and allowed to stand for daughter growth. Subsequent separation of the daughter elements (silver, tellurium, iodine, and lanthanum) provided fission yields for the ^{112}Pd - ^{112}Ag , ^{127}Sb - ^{127}Te , ^{132}Te - ^{132}I , and ^{140}Ba - ^{140}La pairs. Samples of the daughter nuclides (~ 10 mg/ cm^2) were mounted for β counting in calibrated low-background (0.4 counts/min) counting equipment. The radioactive purity of each sample was verified by following its decay. The observed counting rate for each daughter nuclide (extrapolated back to time of separation from the parent) was corrected for its chemical yield and counting efficiency to give the activity of the daughter in equilibrium with the parent at the time of separation. This activity was then corrected for the fission product recoil collection efficiency (50%), chemical yield, decay, genetic relationship, and relative degree of saturation of the parent to give the saturation activity A^∞ of the parent nuclide.

The cumulative fission yield Y is related to A^∞ by the expression

$$Y = A^\infty / \text{fission rate} . \quad (1)$$

The fission rate was estimated from the number of atoms N of ^{257}Fm , the neutron flux ϕ , and the fission cross section σ_f (2950 ± 160 b)²⁹:

$$\text{fission rate} = N\sigma_f\phi . \quad (2)$$

RESULTS AND DISCUSSION

The fission yields determined in this work are presented in Table I with the estimated errors, the number of determinations, and the ratio of the activity found in the sample to the activity found in the blank. This ratio is indicative of fission contamination by $^{235}\text{U}(n,f)$ corresponding to approximately 10^9 atoms of ^{235}U in the dissolved portion of the catcher foil. The average number of neutrons emitted per fission $\bar{\nu}_T$ for $^{257}\text{Fm}(sf)$ is 3.97 ± 0.013 .³⁰ Assuming that $\bar{\nu}_T$ for $^{257}\text{Fm}(n,f)$ is also ~ 4 , symmetric fission is represented by a secondary mass of 127. This is one of the few masses whose yield could be determined and it, together with the yields and reflected yields of the other nuclides, provides a reasonably good representation of the mass distribution from mass 112 through 142 (solid curve in Fig. 3). A smooth extrapolation of the solid curve to masses <112 and >142 was made with the condition that the total fission yield sum to 200%. The results indicate that symmetric mass division is the most probable fission mode for $^{257}\text{Fm}(n,f)$. This is consistent with the provisional mass distribution determined from kinetic-energy measurements of coincident fission fragments⁶ (dashed curve in Fig. 3).

The neutron-emission function for $^{257}\text{Fm}(n,f)$ cannot be determined from the data presented in Fig. 3 by the Terrell method²⁷ of comparing cumulative primary and secondary mass yields, nor is it possible to use the modified method⁷ referred to previously since the latter method requires the application of an assumed $\bar{\nu}(M)$ correction to the kinetic energy data on an event-by-event basis. This cannot be done with the cumulative, provisional data presented in Ref. 6. Even if it could, the resulting mass data must be corrected for mass-dispersive effects associated with target thickness, neutron emission, and the detection system. Such

TABLE I. Fission yields for $^{257}\text{Fm}(n,f)$.

Fission product	Number of determinations	Ratio of sample to blank	Fission yield (%)
$^{140}\text{Ba}(^{140}\text{La})$	2	1.4	3.95 ± 0.60
$^{132}\text{Te}(^{132}\text{I})$	2	1.8	5.57 ± 0.84
$^{127}\text{Sb}(^{127}\text{Te})$	2	11	6.31 ± 0.95
$^{112}\text{Pd}(^{112}\text{Ag})$	2	8	3.02 ± 0.60

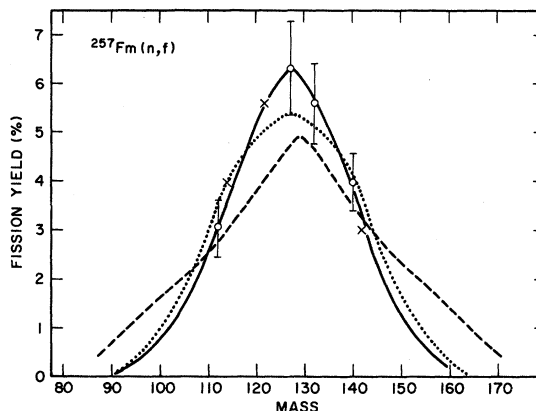


FIG. 3. Secondary mass distribution for $^{257}\text{Fm}(n,f)$. Fission yields measured radiochemically are shown as circles with error flags. Crosses represent reflected yields assuming $\bar{\nu}_T=4$. The solid curve represents the best fit to the data with normalization to 200% total yield. The dotted curve represents the broadest distribution consistent with the errors in the data. Shown for comparison is the provisional mass distribution (dashed curve) determined for $^{257}\text{Fm}(n,f)$ (Ref. 6).

a correction would present a serious problem. Measurements for $^{255}\text{Fm}(n,f)$,⁸ from which the provisional mass distribution in Fig. 1 was obtained, appear to have been subject to considerable dis-

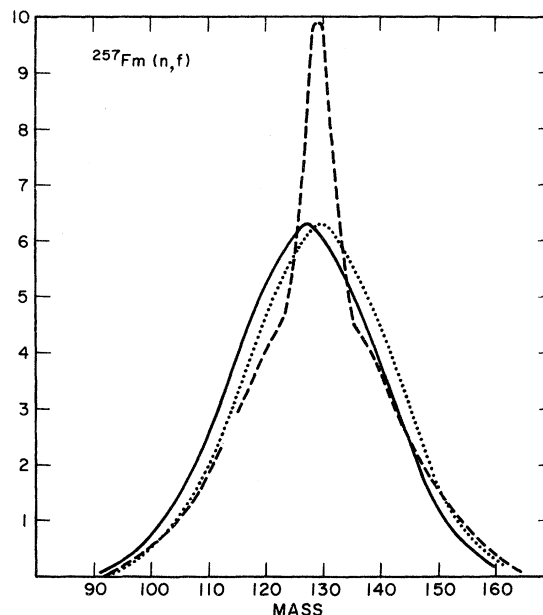


FIG. 4. Primary mass distributions (dotted and dashed curves) derived from the secondary mass distribution (solid curve) by assuming two different neutron yield functions. The dotted curve was obtained by assuming $\bar{\nu}(M)$ to be constant and equal to 2; the dashed curve was obtained by assuming $\bar{\nu}(M)$ to be the same as that deduced for $^{256}\text{Fm}(sf)$ (Ref. 7).

persive effects.³¹ Since the kinetic-energy data for $^{257}\text{Fm}(n, f)^8$ were obtained under similar conditions, it is likely that these data were subject to similar effects. As seen in Fig. 3, the provisional mass distribution (dashed curve) is wider than the secondary mass distribution (solid curve) even if the secondary mass distribution is fitted through the error limits of the radiochemical data (dotted curve).

One may speculate as to the shape of the primary mass distribution if one assumes that the secondary mass distribution is described by the solid curve in Fig. 3 and that $\bar{\nu}(M)$ is some arbitrary function of primary fragment mass subject to the restriction that the average total number of neutrons emitted per fission is equal to 4. If $\bar{\nu}(M)$ is a constant and equal to 2, the primary mass dis-

tribution (dotted curve of Fig. 4) is seen to have the same shape as the secondary mass distribution (solid curve) and is merely displaced by +2 amu. If, however, $\bar{\nu}(M)$ is assumed to be the same as that for $^{256}\text{Fm}(sf)$,⁷ there is a strong peak in the symmetric mass region of the primary distribution (dashed curve). Clearly, more experimental data are required on the $^{257}\text{Fm}(n, f)$ system to establish $\bar{\nu}(M)$ and the exact shape of the mass distribution.

ACKNOWLEDGMENT

The authors wish to thank J. E. Bigelow and the Transuranium Element Production Program at the Oak Ridge National Laboratory for the supply of ^{257}Fm and R. Sjoblom and Dr. E. P. Horwitz for the initial chemical separations of the fermium.

[†]Work performed under the auspices of the U. S. Energy Research and Development Agency.

¹C. F. Tsang and J. B. Wilhelmy, Nucl. Phys. A **A184**, 417 (1972).

²B. D. Wilkins and E. P. Steinberg, Phys. Lett. B **42B**, 141 (1972).

³M. G. Mustafa, U. Mosel, and H. W. Schmitt, Phys. Rev. C **7**, 1519 (1973).

⁴R. Brandt, S. G. Thompson, R. C. Gatti, and L. Phillips, Phys. Rev. **131**, 2617 (1963).

⁵J. P. Balagna, G. P. Ford, D. C. Hoffman, and J. D. Knight, Phys. Rev. Lett. **26**, 145 (1971).

⁶W. John, E. K. Hulet, R. W. Loughheed, and J. J. Weslowski, Phys. Rev. Lett. **27**, 45 (1971).

⁷J. P. Unik, J. E. Gindler, L. E. Glendenin, K. F. Flynn, A. Gorski, and R. K. Sjoblom, in *Proceedings of the Third International Atomic Energy Agency Symposium on the Physics and Chemistry of Fission, Rochester, 1973* (International Atomic Energy Agency, Vienna, 1974), Vol. 2, p. 19.

⁸R. C. Ragaini, E. K. Hulet, R. W. Loughheed, and J. Wild, Phys. Rev. C **9**, 399 (1974).

⁹K. F. Flynn, E. P. Horwitz, C. A. A. Bloomquist, R. F. Barnes, R. K. Sjoblom, P. R. Fields, and L. E. Glendenin, Phys. Rev. C **5**, 1725 (1972).

¹⁰R. M. Harbour, K. W. MacMurdo, D. E. Troutner, and M. V. Hoehn, Phys. Rev. C **8**, 1488 (1973).

¹¹J. C. D. Milton and J. S. Fraser, in *Proceedings of the First Symposium on the Physics and Chemistry of Fission, Salzburg, 1965* (International Atomic Energy Agency, Vienna, 1965), Vol. 2, p. 39.

¹²V. F. Apalin, Yu. N. Gritsyuk, I. E. Kutikov, V. I. Lebedev, and L. A. Mikaelyan, in *Proceedings of the First Symposium on the Physics and Chemistry of Fission, Salzburg, 1965* (see Ref. 11), Vol. 1, p. 587; *Yad. Fiz.* **1**, 639 (1965) [*Sov. J. Nucl. Phys.* **1**, 457 (1965)]; *Nucl. Phys.* **71**, 553 (1965).

¹³V. F. Apalin, Yu. N. Gritsyuk, I. E. Kutikov, V. I. Lebedev, and L. A. Mikaelyan, *Zh. Eksp. Teo. Fiz.*

46, 1197 (1964) [*Sov. Phys.—JETP*, **46**, 810 (1964)]; *Nucl. Phys.* **55**, 249 (1964).

¹⁴J. S. Fraser and J. C. D. Milton, *Annu. Rev. Nucl. Sci.* **16**, 379 (1966).

¹⁵T. Cornell, E. E. Maslin, and A. L. Rodgers, in *Proceedings of the First Symposium on the Physics and Chemistry of Fission, Salzburg, 1965* (see Ref. 11), Vol. 2, p. 67.

¹⁶E. E. Maslin, A. L. Rodgers, and W. G. F. Core, *Phys. Rev.* **164**, 1520 (1967).

¹⁷J. W. Boldeman, A. R. de L. Musgrove, and R. L. Walsh, *Aust. J. Phys.* **24**, 821 (1971).

¹⁸S. L. Whetstone, *Phys. Rev.* **114**, 581 (1959).

¹⁹H. R. Bowman, J. C. D. Milton, S. G. Thompson, and W. J. Swiatecki, *Phys. Rev.* **129**, 2133 (1963).

²⁰E. Nardi and Z. Fraenkel, *Phys. Rev. Lett.* **20**, 1248 (1968).

²¹A. Gavron and Z. Fraenkel, *Phys. Rev. Lett.* **27**, 1148 (1971); *Phys. Rev. C* **9**, 632 (1974).

²²C. Signarbieux, J. Poitou, M. Ribrag, and J. Matussek, *Phys. Lett. B* **39B**, 503 (1972).

²³C. Signarbieux, H. Nifenecker, J. Poitou, and M. Ribrag, *J. Phys. (Paris) Suppl.* **33**, C5-1-23 (1972).

²⁴C. Signarbieux, R. Babinet, H. Nifenecker, and J. Poitou, in *Proceedings of the Third International Atomic Energy Agency Symposium on the Physics and Chemistry of Fission, Rochester, 1973* (see Ref. 7), Vol. 2, p. 117.

²⁵K. F. Flynn, J. E. Gindler, and L. E. Glendenin, (unpublished).

²⁶K. Flynn, J. Gindler, L. Glendenin, A. Gorski, R. Sjoblom, and J. Unik, in *Abstracts of Papers, 167th National Meeting, American Chemical Society, Los Angeles, California, March 31–April 5, 1974* (Port City Press, Baltimore, 1974), No. NUCL-22.

²⁷J. Terrell, *Phys. Rev.* **127**, 880 (1962); in *Proceedings of the First Symposium on the Chemistry and Physics of Fission, Salzburg, 1965* (see Ref. 11), Vol. 2, p. 3.

²⁸E. P. Horwitz and C. A. A. Bloomquist, *J. Inorg. Nucl. Chem.* 35, 271 (1973).

²⁹J. F. Wild, E. K. Hulet, and R. W. Lougheed, *J. Inorg. Nucl. Chem.* 35, 1063 (1973).

³⁰E. Cheifetz, H. R. Bowman, J. B. Hunter, and S. G. Thompson, *Phys. Rev. C* 3, 2017 (1971).

³¹K. F. Flynn, J. E. Gindler, R. K. Sjoblom, and L. E. Glendenin, *Phys. Rev. C* 11, 1676 (1975).